Reconnection of MV Microgrid with Universal Grid-forming Inverter-based Resources

RECONNECTION OF MV MICROGRID WITH UNIVERSAL GRID-FORMING INVERTER-BASED RESOURCES

Hannu Laaksonen[1*] and Nikos Hatziargyriou[2]

[1]*School of Technology and Innovations, University of Vaasa, Vaasa, Finland*
[2]*School of Electrical and Computer Engineering, National Technical University of Athens, Athens, Greece*
hannu.laaksonen@uwasa.fi

Keywords: GRID-FORMING, CONTROL, MICROGRID, ISLANDING, RECONNECTION, STABILITY, SYNCHRONIZATION

Abstract

One concern of typically proposed grid-forming (GFM) inverter-based resources (IBRs) has been the microgrid reconnection i.e. transition from islanded to grid-connected operation. Therefore, this paper presents a case study about medium-voltage (MV) microgrid reconnection with universal frequency-locked-loop (U-FLL) -based GFM IBRs. The main aim of the PSCAD simulations was to find out that what is the maximum allowed voltage phase angle difference before MV microgrid reconnection to maintain stability of U-FLL-based IBRs after the reconnection and how much it is dependent on the simultaneous frequency and voltage magnitude differences. Based on the simulation results, the U-FLL based IBRs have very good voltage phase angle difference ride through capabilities i.e. ±140-180° depending on the case. Paper also proposes one new scheme in which perfectly synchronized reconnection could be always achieved by having U-FLL input of one MV IBR from a utility grid synchronous generator's rotating speed. In addition, paper presents further modified and improved U-FLL-based synchronization method which is grid-forming for generating IBRs and grid-supporting for IBR-based loads.

1 Introduction

In the future, the IBRs must be increasingly capable to operate stably during different type of operation modes, events and faults. Also, the fault behaviour and response of the IBRs needs to be compatible with the network protection and islanding detection schemes. The main control schemes of IBRs can be divided into GFM and grid-following (GFL) ones that typically behave differently during disturbances and rapid changes mainly due to differences in their synchronization. However, in the future the amount of GFM IBRs must be increased to guarantee stability of the power system also during topology changes and transitions between normal grid-connected and islanded operation. [1]-[3]

Multiple different control schemes for GFM IBRs have been proposed and it has been stated, for example, in [4] that commonly proposed GFMs suffer greater impacts from faults in strong grids and GFLs in weak grids. In [5], it was also notified that the typical GFM IBR control methods can have challenges related to, angle stability, fault-ride-through (FRT) capability, and transition from islanded to grid-connected mode (i.e. microgrid reconnection). The unintentional islanding of commonly proposed GFM IBRs has also been seen as a risk to the reliability of future IBR-based power systems, because the variables that are used for islanding detection of GFMs are different than with GFLs. [6]-[8]

Microgrid reconnection from islanded to grid-connected operation can potentially lead to large oscillations due to the possible difference between microgrid and utility grid frequency, voltage phase angle and voltage magnitude. These deviations are always challenging for synchronous generators (SGs), but they can be also challenging for the post transition stability of GFM IBRs after the reconnection. Therefore, different coordinated control schemes that can enable synchronized reconnection and minimize frequency, phase angle and magnitude differences before microgrid reconnection has been proposed in the literature. [5], [9]

In HV transmission network synchronism check relays can be, for example, configured so that frequency difference should be under 0.055 Hz and voltage phase angle difference 20° - 45° before closing the circuit-breaker [10]. On the other hand, regarding LV microgrids it has been stated in [9] and [11] that the voltage phase angle difference should be less than 60° before microgrid reconnection and depending on the IBR synchronization scheme it could be also a bit higher [12]. However, with SGs the phase difference should be preferably significantly smaller than 60°, even less than 10°, to avoid large oscillations and electrical and mechanical stresses [9]. Based on [13] microgrid re-synchronizing function must meet a more stringent requirement than the one defined by IEEE 1547 which requires that the phase difference between microgrid and utility grid should less than 20° before the microgrid connection point circuit-breaker can close. Different standards and grid codes increasingly also define phase angle jump ride through requirements for IBRs and especially for GFM IBRs. Based on [14] a sudden voltage phase angle jump can result in the GFM IBR to lose synchronization and control stability. For example, IEEE 1547-2018 [15] defines the voltage phase angle jumps withstand / ride-through requirements for multi-phase distributed energy resources (DERs) to be ≤ 20°. On the other hand, IEEE Standard 2800–2022 [16] states that any IBR should be able to ride through a voltage phase angle change of ± 25°. It has been also notified in [17] that in reality (not related to microgrid reconnection) even 50° phase angle jumps can occur and that, for example, synchrophasor measurement units (PMUs) are only tested for phase jumps of +/-10° [18]. In [17] it was also stated that traditional GFL IBRs that are synchronized with phase-locked-loops (PLLs) are sensitive to react to phase angle jumps. Therefore, utilization of robust and stable U-FLL instead of PLL could be also of importance in the future.

This paper studies by PSCAD simulations that what is the maximum allowed voltage phase angle difference before MV microgrid reconnection and how much it is dependent on the simultaneous frequency and voltage magnitude differences. This means that the focus of this paper is not on different control schemes which can enable synchronized and seamless microgrid reconnection like in [5] and [9]. However, the paper proposes also one new scheme in which perfectly synchronized reconnection could be always achieved by having U-FLL input of one MV IBR from a utility grid synchronous generator's rotating speed. In addition, further modified and improved U-FLL from [2], [3], [7] and [8] is presented in the paper.

2. Study System

The simulation studies are done with simplified HV/MV/LV network PSCAD model, like in [20] and [21], including active DER units in the MV network (1 MW PV, 2 MW BESS, 1 MW EV charging station) and in the LV network (0.45 MW PV, 0.2 MW BESS) as well as OLTCs at HV/MV and MV/LV substations as shown in Fig. 1.

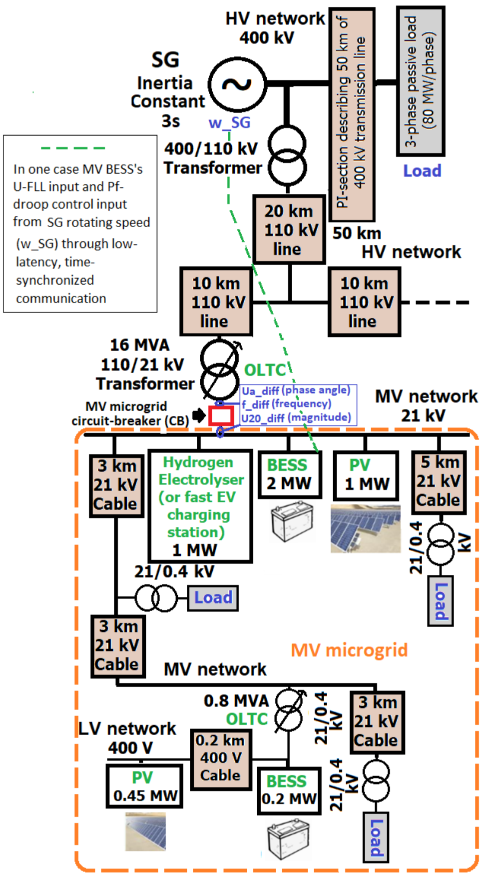

Fig. 1. Study system with MV microgrid.

Fig. 2 presents the MV BESS's average PSCAD model with controlled voltage sources and related control scheme with U-FLL based synchronization.

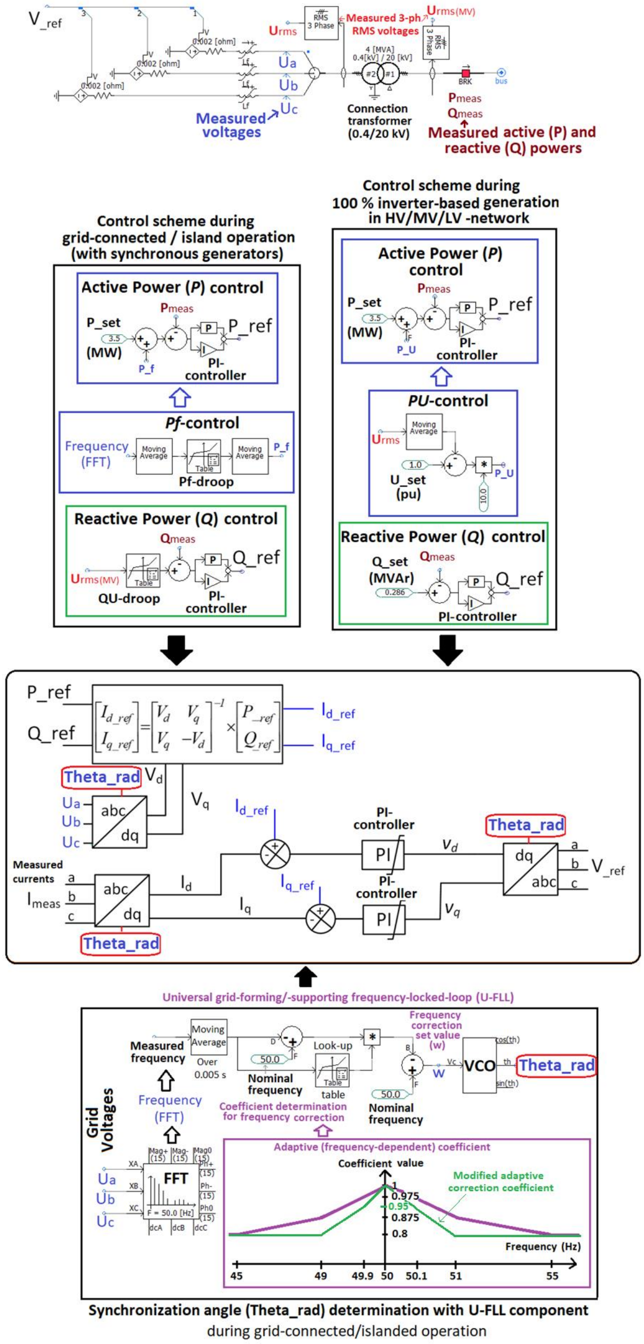

Fig. 2. MV BESS's average PSCAD model with controlled voltage sources and related control scheme with U-FLL based synchronization (see Fig. 1 and 3). [19]

In the previous studies [2], [3], [7] and [8] U-FLL-based grid-forming and -supporting synchronization method, which can directly replace the phase-locked-loop (PLL) -component of GFL inverters, has been proposed and simulated with multiple type of DERs. U-FLL-based synchronization method [2] is grid-forming for inverter-based generating units and grid-supporting for inverter-based loads. This paper presents case studies with PSCAD simulations in which the reconnection of MV microgrid with U-FLL based DER units is studied. In this paper, the studied MV microgrid is 100 % U-FLL and IBR-based (Fig. 1) i.e. it does not have any SGs. In 100 % IBR-based MV microgrid without any SGs, the *Pf*-control of the DER units' (Fig. 1) is disabled and the BESSs and EV charger/hydrogen electrolyzer are changed to *PU*-control mode during the island operation (Fig. 2). Transition to *PU*-control takes place instantly after islanding detection [7].

In [2] it was mentioned that U-FLL and other GFM schemes should be also stable during long duration frequency deviations and in [19] an enhanced U-FLL with phase angle difference monitoring was presented. In this paper, further modified U-FLL is used (Fig. 3) with different limiters during normal and 3-phase faults with sample and hold-logic to ensure transient stability [8] as well as stability ensuring U-FLL internal phase difference monitoring block with reference from U-FLL with coefficient 1 (instead of PLL as in [19]).

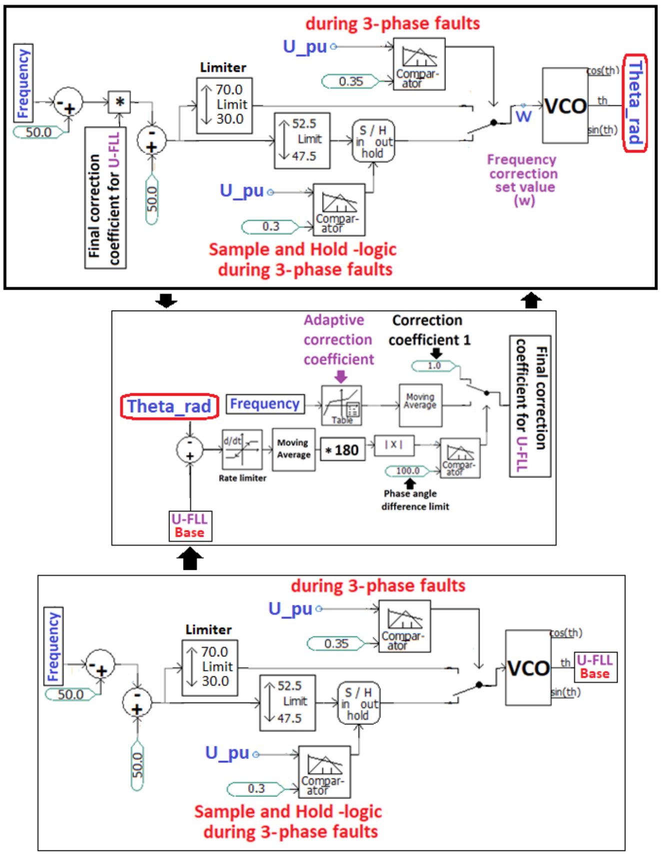

Fig. 3. Further modified U-FLL with different limiters during normal and 3-phase faults with sample and hold-logic as well as stability ensuring U-FLL internal phase difference monitoring block with reference from U-FLL with coefficient 1 (see also Fig. 2).

The main purpose of the PSCAD simulations of this paper was to find out that what is the maximum allowed voltage A phase angle difference (*Ua_diff*) between MV microgrid and utility grid (Fig. 1) before MV microgrid reconnection with U-FLL based IBRs to maintain stability after the reconnection. In addition, the effect of simultaneous frequency difference (*f_diff*) and voltage magnitude/amplitude difference (*U20_diff*) was considered. Fig. 1 shows the urban MV network model with MV cables and MV DER units' directly at the HV/MV substation. Only DER average models with U-FLL, similar to Fig. 2 and the models in [2], [3], [7], [8] and [19] are used in this paper. However, in previous studies [2], [3], [7] and [8] the conclusions related to detailed IBR-based models with U-FLL have been similar to the conclusions with the average IBR models.

3 Simulations

The differences of the main simulation study cases of this paper are summarised in Table 1 and the used simulation sequence in Table 2. Before MV microgrid reconnection i.e. transition back to utility grid-connected mode from islanding (Table 2, Fig. 1) also voltage magnitude difference (*U20_diff*) between microgrid and utility grid could be reduced by MV BESS *PU*-control, but it is not done to find out the maximum allowed voltage phase angle difference for stable microgrid reconnection.

Table 1. Main study cases.

Case	*PU*-control's *U*-target/set value (pu) of MV DER*)	*PU*-control's *U*-target/set value (pu) of LV BESS	U-FLL input frequency°) of DER
CASE_1A	1.0	1.0	FFT
CASE_1B	1.0	1.0	Freq. meas. **)
CASE_2	1.05	1.0	FFT
CASE_3	1.1	1.1	FFT
CASE_4	1.0	1.0	FFT / SG rotating speed***)

*) MV BESS and MV EV charger/hydrogen electrolyzer (Fig. 1 and 2), **) Each zero-crossing of the 3-phase input voltage is tracked and used to calculate 6 time intervals, ***)With MV BESS (Fig. 1), °)See Fig. 2 and 3

Table 2. Simulation sequence.

Time (*t*)	Event
19.9	HV network load increase
20.0	MV network microgrid islanding (Fig. 1)
50.0	HV and MV network (during MV islanding) load increase
50-100	MV network microgrid reconnection (Fig. 1)

Table 3 summarizes the results of multiple simulations. It shows the maximum allowed phase A voltage phase angle difference *Ua_diff* for stable MV microgrid reconnection (Fig. 1 and Table 1 & 2) and simultaneous values of frequency difference *f_diff* and voltage magnitude difference *U20_diff* (across MV microgrid circuit-breaker) in the main study cases 1-3 (Table 1).

Table 3. Maximum allowed phase A voltage phase angle difference *Ua_diff* for stable MV microgrid reconnection (Fig. 1 and Table 1 & 2) and simultaneous values of frequency difference *f_diff* and voltage magnitude difference *U20_diff* (across MV microgrid circuit-breaker at the moment of microgrid reconnection) in study cases 1-3 (Table 1).

	CASE_1A	CASE_1B	CASE_2	CASE 3
Ua_diff (degrees)	+140°	-146°	-160°	+180°
f_diff (Hz)	0.01	0.03	0.0	0.09
U20_diff (pu)	0.0566	0.059	0.015	-0.026
MG reconnection time *t* (s)	92.47	53	57.6	52.913

It can be concluded from Table 3 results that higher *PU*-control target value of MV DERs (Table 1) allows also larger maximum *Ua_diff* value for stable MV microgrid reconnection. However, it should be noted that the voltage magnitude difference *U20_diff* across MV microgrid circuit-breaker is larger in CASE_1A and CASE_1B which affects to the maximum allowed *Ua_diff* value. In addition, based on the simulation results of CASE_1A and CASE_1B (Table 1 and 3) the U-FLL input frequency of DER can also have a slight impact on maximum allowed *Ua_diff* value for stable MV microgrid reconnection. In CASE_3 *f_diff* is larger at the moment of MV microgrid reconnection but still it has the largest allowed *Ua_diff* value (Table 3). Tables 4 and 5 present also as an example few unstable subcases from CASE_1A (Table 4) and CASE_1B (Table 5). Table 5 (CASE_1B) shows that a subcase with smaller +130° *Ua_diff* value is also unstable when both *f_diff* and *U20_diff* values were higher than in the stable CASE_1B subcase with -146° *Ua_diff* value (Table 5).

Table 4. *Ua_diff, f_diff* and *U20_diff* values in CASE_1A (Table 1 and 3).

	Ua_diff (degrees)	*f_diff* (Hz)	*U20_diff* (pu)	Stable (Yes/No)
CASE_1A	+160°	0.01	0.058	No
	+150°	0.01	0.0574	No
	+140°	0.01	0.0566	Yes

Table 5. *Ua_diff, f_diff* and *U20_diff* values in CASE_1B (Table 1 and 3).

	Ua_diff (degrees)	*f_diff* (Hz)	*U20_diff* (pu)	Stable (Yes/No)
CASE_1B	+160°	0.21	0.053	No
	+130°	0.435	0.058	No
	-146°	0.03	0.059	Yes

Based on the simulation results, the U-FLL based IBRs have very good voltage phase angle difference (*Ua_diff*, Fig. 1) or phase jump ride through / withstand capabilities i.e. depending on the case ± 140-180°. That is much more than defined e.g. by IEEE 1547 [13] which requires that the phase difference between microgrid and utility grid should less than 20° before the reconnection or by IEEE 1547-2018 [15] which defines the voltage phase angle jumps withstand / ride-through requirements for multi-phase DERs must be ≤ 20°. IEEE Standard 2800–2022 [16] requires also that any IBR should be able to ride through a voltage phase angle change of ± 25°.

In Fig. 4 and 5, active power *P* and reactive power *Q* behaviour of MV DER units (BESS, PV, EV/Electrolyzer, see Fig. 1) as well as MV microgrid and utility grid frequency at the moment of MV microgrid reconnection are presented from the main study cases (Table 1) CASE_1A (Fig. 4) and CASE_3 (Fig. 5) with maximum allowed *Ua_diff* for stable MV microgrid reconnection (Table 3). The oscillations in *P* and *Q* of MV DER units (Fig. 4a), 4b), 5a) and 5b) are due to large *Ua_diff* value before the reconnection. In addition, for example, change in *P* and *Q* of MV BESS after the microgrid reconnection in Fig. 4b) and 5b) takes place also due to the control method change back to grid-connected mode control (Fig. 2).

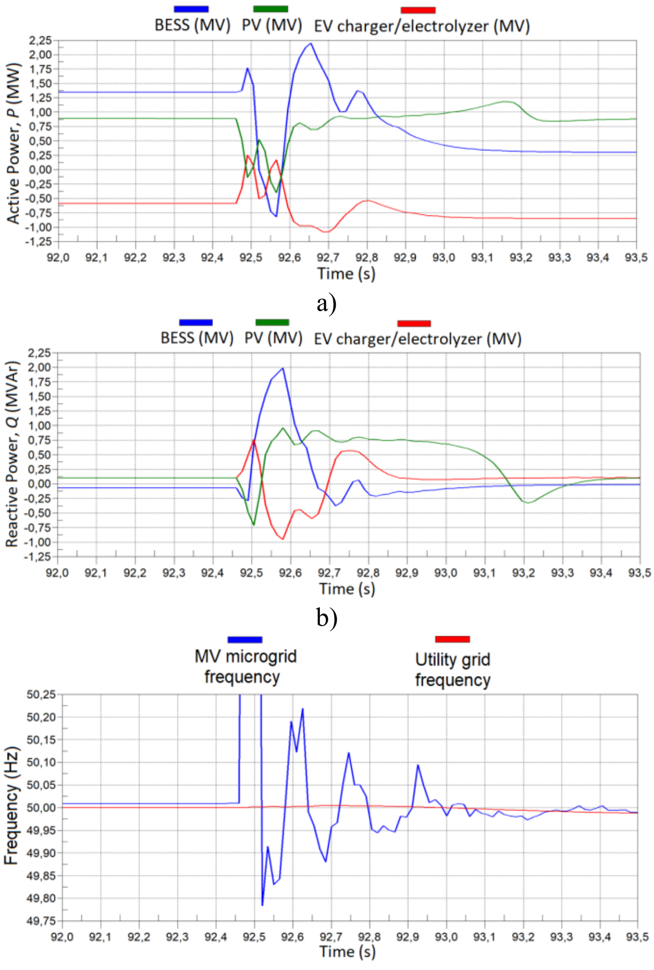

Fig. 4. CASE_1A (Table 1 and 3) a) active power *P* and b) reactive power *Q* behavior of MV DER units (BESS, PV, EV/Electrolyzer) as well as c) MV microgrid and utility grid frequency at the moment of MV microgrid reconnection at *t*=92.47 s (see also Fig. 1).

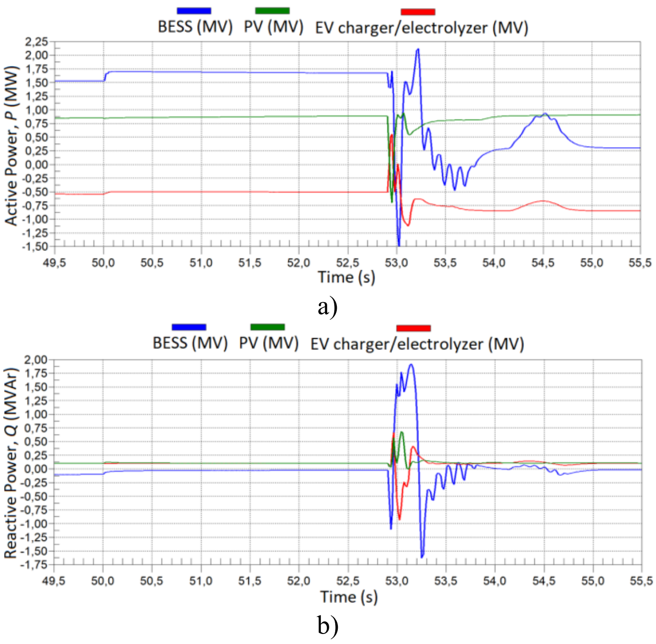

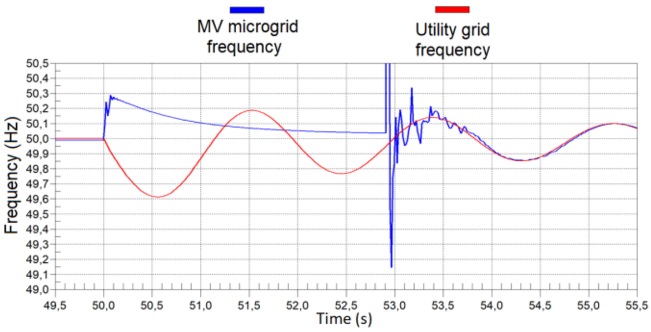

c)

Fig. 5. CASE_3 (Table 1 and 3) a) active power *P* and b) reactive power *Q* behavior of MV DER units (BESS, PV, EV/Electrolyzer) as well as c) MV microgrid and utility grid frequency at the moment of MV microgrid reconnection at *t*=52.913 s (see also Fig. 1 and simulation seq. in Table 2).

Fig. 6 presents simulation results from the main study case CASE_4 (Table 1).

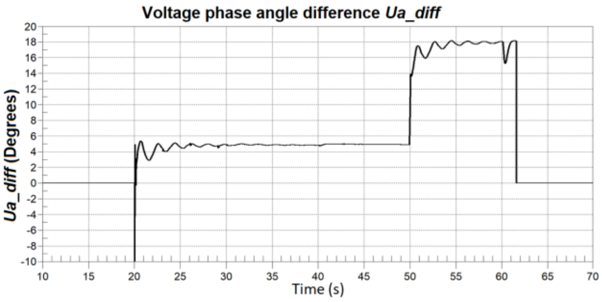

a)

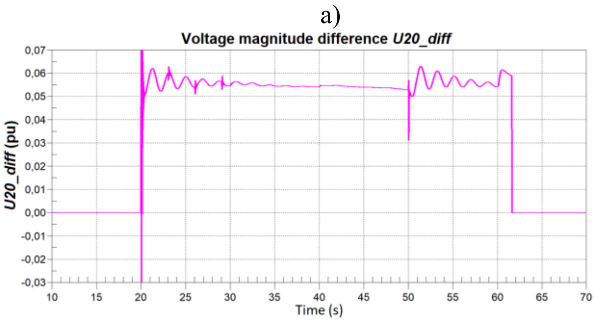

b)

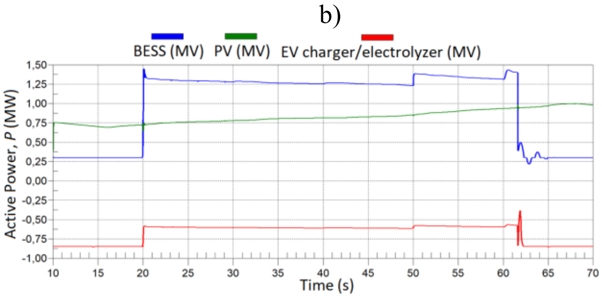

c)

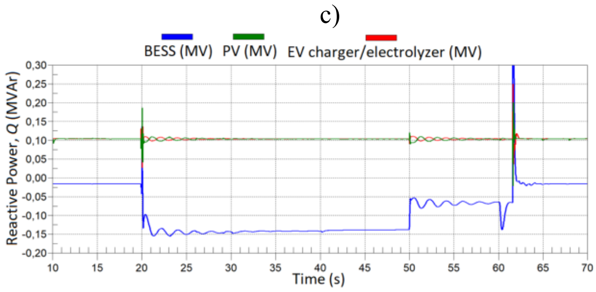

d)

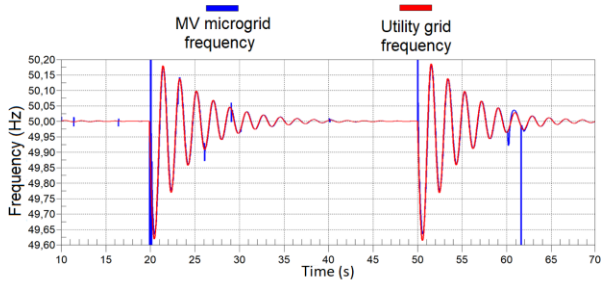

e)

Fig. 6. CASE_4 (Table 1 and 3) a) voltage phase angle difference *Ua_diff*, b) voltage magnitude difference *U20_diff*, c) active power *P* and d) reactive power *Q* behavior of MV DER units (BESS, PV, EV/Electrolyzer) as well as e) MV microgrid and utility grid frequency (MV microgrid reconnection at *t*=61.59 s, see also Fig. 1 and simulation sequence in Table 2).

Fig. 6 shows voltage phase angle difference *Ua_diff,* voltage magnitude difference *U20_diff*, active and reactive power behavior of MV DER units (BESS, PV, EV/Electrolyzer, see Fig. 1) as well as MV microgrid and utility grid frequency from CASE_4 in which U-FLL input of one MV DER (MV BESS, Fig. 1) comes directly from utility grid SG's rotating speed (w_SG Fig. 1) through time synchronized, low-latency communication. It can be seen from the simulation results of CASE_4, (Fig. 6) that perfectly synchronized reconnection could be always achieved by only having U-FLL input of one MV DER (MV BESS, Fig. 1) from utility grid SG's rotating speed (*w_SG* Fig. 1) with time synchronized, low-latency communication. Potentially U-FLL input could also be from utility grid side frequency. It can be also seen from Fig. 6e) that utility grid frequency fluctuations are also seen in this CASE_4 on MV microgrid's frequency and further as small simultaneous oscillations in reactive powers of MV DER units (Fig. 6d). In principle, during microgrid island operation BESS U-FLL input could be changed to come from utility grid frequency or SG's speed to always ensure microgrid's smooth and seamless reconnection. However, the input change should be done when the measured voltage phase difference is small enough in order to prevent U-FLL based IBRs' control instability. Regarding microgrid reconnection, focus should be also on stability of IBR-/converter connected loads after reconnection. Use of U-FLL-based synchronization on IBR-based loads could also support their stability after the microgrid reconnection as shown by the simulations.

4 Conclusions

Different control schemes based on communication utilisation could be applied to enable synchronized and seamless microgrid reconnection e.g. [5] and [9], but the focus of this paper was to study that what is the maximum allowed voltage phase angle difference (*Ua_diff*) before stable MV microgrid reconnection (e.g. in case communication for resynchronization is not available or is unreliable) and how much it is dependent on the simultaneous frequency (*f_diff*) and voltage magnitude (*U20_diff*) differences with U-FLL based IBRs in 100 % IBR-based MV microgrid. However, the paper presented also a new scheme in which perfectly synchronized reconnection could be always achieved by having the U-FLL input of one MV DER (MV BESS, Fig. 1) from utility grid SG's rotating speed (*w_SG*) with time synchronized, low-latency communication (potentially U-FLL input could also be from utility grid side frequency). The paper also presented further modified U-FLL with different limiters during normal and 3-phase faults with sample and hold-logic as well as stability ensuring U-FLL internal phase difference monitoring block with reference from U-FLL with coefficient 1. This further modified U-FLL-based synchronization which is grid-forming for generating IBRs and grid-supporting for IBR-based loads showed very stable operation in all different kind of disturbances and fluctuations.

Simulation results showed that the U-FLL-based IBRs used in this paper (i.e. modelled with average voltage sources) had very good voltage phase angle difference ride through capabilities i.e. stable MV microgrid reconnection was possible with ±140-180° angle difference depending on the case. Based on the results higher *PU*-control target value of MV DERs could allow a bit larger maximum *Ua_diff* value for stable MV microgrid reconnection if it simultaneously reduces *U20_diff* value and *f_diff* value also remains reasonably low at the moment of MV microgrid reconnection. As a conclusion from simulations with a presented new scheme in which U-FLL input of one MV DER comes from utility grid SG's rotating speed it can be stated that reconnection is always successful and it is enough to have utility grid SG's speed (or measured frequency) as an input for only one MV DER (MV BESS in this case). Local frequency measurement-based operation could be used as a back-up if communication fails. However, this new scheme works only in case of 100 % U-FLL- and IBR-based microgrid and is not possible if there is a SG inside microgrid during the island operation. In this kind of hybrid microgrid with IBRs and SGs only local frequency measurement-based control should be used.

In general, the utilization of U-FLL based DERs could improve the resiliency of the future IBR-based power systems. However, it could be noted that only DER average models with U-FLL were used in this paper and results should be also confirmed in further studies with detailed IBR-based models with U-FLL as well as with hardware-in-the-loop simulations.

5 Acknowledgements

This work has been done as a part of "Smart Grid 2.0" - project funded by Business Finland with grant No. 1386/31/2022.

6 References

[1] Tuohy, A., Dattaray, P., Farantatos, E., Kelly, A., Lannoye, E.: Implications of Reduced Inertia Levels on the Electricity System: Technical Report on the Challenges and Solutions for System Operations with Very High Penetrations of Non-Synchronous Resources, EPRI, Palo Alto, CA, 2019

[2] Laaksonen, H.: 'Universal Grid-forming Method for Future Power Systems', IEEE Access, 2022

[3] Laaksonen, H.: 'Improvement of Power System Frequency Stability with Universal Grid-forming Battery Energy Storages', IEEE Access, 2023

[4] Hadjileonidas, A., Li Y., Green, T. C.: 'Comparative Analysis of Transient Stability of Grid-Forming and Grid-Following Inverters', Proc. IEEE PEAC-conference, 2022

[5] Rosso, R., Wang, X., Liserre, M., Lu, X., Engelken, S.: 'Grid-Forming Converters: Control Approaches, Grid-Synchronization, and Future Trends—A Review', IEEE Open Journal of Industry Applications, 2021, 2, pp. 93-109

[6] Liu, T., Wang, X., Liu, F., Xin, K., Liu, Y.: 'Islanding Detection of Grid-Forming Inverters: Mechanism, methods, and challenges', IEEE Electrification Magazine, 2022, 10

[7] Laaksonen, H.: 'Islanding Detection with Universal Grid-forming Inverter-based Generation', Proc. CIRED 2023, Rome, Italy, 2023

[8] Laaksonen, H.: 'Solutions to Improve Transient Stability of Universal Grid-forming Inverter-based Resources', Int. Review of Electrical Engineering (IREE), 2023, 18, 3

[9] Laaksonen, H., Kauhaniemi, K.: 'Synchronized re-connection of island operated LV microgrid back to utility grid', Proc. IEEE PES Innovative Smart Grid Technologies Conference Europe (ISGT Europe), Gothenburg, Sweden, 2010

[10] AREVA T&D, Network Protection & Automation Guide, First edition, July 2002

[11] Oyarzabal, J. et al.: Report on applied data structures and mapping to communication means, WPE: Standardization of technical and commercial protocols and hardware, More MicroGrids, 2009

[12] Laaksonen, H. Kauhaniemi, K.: 'Smart Protection Concept for LV Microgrid', Int. Review of Electrical Engineering (IREE), 2010

[13] Eto, J. et al.: 'Overview of the CERTS Microgrid Laboratory Test Bed', Proc. Integration of Wide-Scale Renewable Resources Into the Power Delivery System, CIGRE/IEEE PES Joint Symposium, Calgary, Canada, 2009

[14] Lin T., Das, M. Gole, A., Isaacs, A.: 'Adaptive fault ride through control of VSM Grid-forming converters', Electric Power Systems Research, 223, 2023, 109606

[15] IEEE Standard for Interconnection and Interoperability of Distributed Energy Resources With Associated Electric Power Systems Interfaces, Standard IEEE 1547-2018, IEEE Standards Association, IEEE Standards Coordinating Committee 21, 2018

[16] IEEE standard for interconnection and interoperability of inverter-based resources (IBRs) interconnecting with associated transmission electric power systems, IEEE Std 2800-2022, 2022

[17] Bumiller, G.: Technology for Robust, Low-Latency Frequency and Phasor Estimation and Evaluation with a Real HV Short-Circuit Event', Proc. CIRED 2024 Workshop on Increasing Distribution Network Hosting Capacity, Vienna, Austria, 2024

[18] IEEE/IEC International Standard 60255-118-1 - Measuring relays and protection equipment - Part 118-1:
Synchrophasor for power systems - Measurements, USA, 2018

[19] Laaksonen, H.: 'Stability of Future Low-Inertia Power Systems with Different Grid-Forming Control Schemes', Proc. CIRED 2024 Workshop on Increasing Distribution Network Hosting Capacity, Vienna, Austria, 2024

[20] Laaksonen, H., Khajeh, H., Hatziargyriou, N.: 'Novel DER and OLTC Management Scheme for Coordinated TSO-DSO Flexibility Services Provision', Proc. ISGT Europe, Grenoble, France, 2023

[21] Laaksonen, H., Khajeh, H., Hatziargyriou, N.: 'Coordinated Control Schemes for Improved DER Hosting Capacity and Flexibility Provision', Proc. CIRED 2024 Workshop on Increasing Distribution Network Hosting Capacity, Vienna, Austria, 2024